

Damping Heat Coefficient – Theoretical and Experimental Research on a Vibrating Beam

Cite as: Journal of Sound and Vibration, Volume 400, 21 July 2017, Pages 1321, DOI:10.1016/j.jsv.2017.04.023

Marko Mihalec^a, Jaka Javh^a, Filippo Cianetti^b, Michele Moretti^b, Gianluca Rossi^b, Janko Slavič^{a,*}, Miha Boltežar^a

^a *University of Ljubljana, Faculty of Mechanical Engineering, Aškerčeva 6, 1000 Ljubljana, Slovenia*

^b *University of Perugia, Department of Engineering, via Duranti 93, 06125 Perugia, Italy*

Abstract

Vibrating systems dissipate their vibrational energy through different mechanisms, commonly referred to as damping. Damping converts the vibrational energy into other forms, such as heat and sound radiation. Heating of the material is often assumed to be one of the biggest drains of energy; however, the measurable temperature increase is at the level of milli Kelvin and hard to measure. This research introduces a damping heat coefficient, the coefficient of total dissipated energy that is converted into heat. Using this coefficient, the expected temperature change of a beam is theoretically related to its damping ratio. In addition, the damping heat coefficient is determined experimentally by measuring the temperature increase of a vibrating beam. Based on modal damping, it is shown that different amounts of energy are

*Corresponding author: janko.slavic@fs.uni-lj.si, +386 1 4771 226, fax:+386 1 2518 567

dissipated at different parts of the structure. The numerical heat model was experimentally confirmed.

1. Introduction

Damping is a phenomenon that dissipates the energy of every vibrating system. Depending on its spatial origin, damping can be classified as material damping, boundary damping and damping due to fluid-structure interactions [1]. This paper focuses on material damping, which mainly encompasses thermoelastic damping and internal friction [2, 3].

From the macroscopic standpoint, damping is often categorized as either hysteretic or viscous damping [4, 5]. Viscous damping is especially characteristic of cases where the observed structure is made of polymeric material [6].

Regardless of the mechanism, damping dissipates the vibrational energy into other forms, such as the energy of sound waves and heat. Since different damping mechanisms ultimately result in the generation of heat, this research focuses on measuring the temperature increase as a result of damping.

While damping is of interest when studying any vibrating system, the relation between damping and its thermal effects has not been widely researched [7], especially due to the small temperature changes that are difficult to measure. When investigating thermoelastic damping, Norris and Photiadis [8] related the thermal loss and the principal curvatures in thin plates.

The manuscript is organized as follows. Section 2 introduces the theoretical backgrounds that relate the damping of a vibrating beam to the temperature increase. In Section 3, the experiment that was carried out to

validate the theoretical backgrounds is presented. Section 4 presents the results by firstly examining the predicted and measured spatial temperature increase and, secondly, determining the fraction of dissipated energy that was converted to heat (*i.e.*, the damping heat coefficient). The last section draws the conclusions.

2. Theoretical background

2.1. Damping according to the Kelvin-Voigt material model

One way to model the damping in materials is to use the Kelvin-Voigt viscous material model [9], where a viscous damper and an elastic spring are connected in parallel, see Fig. 1:

$$\sigma(t) = E \varepsilon(t) + \eta \frac{\partial \varepsilon(t)}{\partial t} \quad (1)$$

where $\sigma(t)$ is the stress in the material, $\varepsilon(t)$ is the strain in the material, E is the modulus of elasticity and η is the viscosity.

By using the Euler-Bernoulli beam theory, the strain in the beam is modeled as [9, 10]:

$$\varepsilon(x, z, t) = -z \frac{\partial^2 w(x, t)}{\partial x^2}, \quad (2)$$

where z is the coordinate from the beam center in the direction of the beam's thickness and $w(x, t)$ is the beam deflection. The shear was neglected; therefore, the stress is assumed to be uniaxial according to Eq. (2) and via Eq. (1) produces:

$$\sigma(x, z, t) = E \left(-z \frac{\partial^2 w(x, t)}{\partial x^2} \right) + \eta \left(-z \frac{\partial^3 w(x, t)}{\partial x^2 \partial t} \right) \quad (3)$$

where only the second, viscous term is responsible for the damping.

If the beam is excited at or close to a natural frequency ω , the corresponding

deflection shape $\phi(x)$ defines the motion of the beam [11]:

$$w(x, t) = \text{Re}\{\phi(x)\} \cos(\omega t) + \text{Im}\{\phi(x)\} \sin(\omega t) \quad (4)$$

By deriving the beam deflection (4) over time and implementing it in the viscous part of Eq. (3) the stress caused by the material's viscosity is:

$$\sigma_d(x, z, t) = \eta z \omega \left(\frac{\partial^2 \text{Re}\{\phi(x)\}}{\partial x^2} \sin(\omega t) - \frac{\partial^2 \text{Im}\{\phi(x)\}}{\partial x^2} \cos(\omega t) \right) \quad (5)$$

The differential energy dW_d lost to damping equals the viscous force F_d over the displacement dx :

$$dW_d = F_d dx, \quad (6)$$

or in terms of material stress and strain for a finite volume ΔV :

$$dW_d = (\sigma_d \Delta A) (\Delta l d\varepsilon) = \sigma_d d\varepsilon \Delta V \quad (7)$$

By deriving the damped energy W_d (7) with regards to time t and omitting the finite volume ΔV , the volumetric damping power caused by the beam's viscosity is introduced as:

$$P_{d\Delta V}(x, z, t) = \sigma_d(x, z, t) \frac{\partial \varepsilon(x, z, t)}{\partial t} \quad (8)$$

Using Eqs. (2), (4) and (5) with the volumetric damping power (8) the result is:

$$P_{d\Delta V}(x, z, t) = \eta \omega^2 z^2 \left[\left(\frac{\partial^2 \text{Re}\{\phi(x)\}}{\partial x^2} \right)^2 \sin^2(\omega t) + \left(\frac{\partial^2 \text{Im}\{\phi(x)\}}{\partial x^2} \right)^2 \cos^2(\omega t) - 2 \left(\frac{\partial^2 \text{Re}\{\phi(x)\}}{\partial x^2} \right) \left(\frac{\partial^2 \text{Im}\{\phi(x)\}}{\partial x^2} \right) \sin(\omega t) \cos(\omega t) \right] \quad (9)$$

By neglecting the power oscillations with 2ω , resulting from the squares and multiplications of the trigonometric functions and observing the damping power quasi-statically over time

$$\sin^2(\omega t) = \frac{1}{2} \left(\cos(0) - \cos(2\omega t) \right) \xrightarrow{qs} \frac{1}{2} \quad (10)$$

$$\cos^2(\omega t) = \frac{1}{2} \left(\cos(0) + \cos(2\omega t) \right) \xrightarrow{qs} \frac{1}{2} \quad (11)$$

$$\sin(\omega t) \cos(\omega t) = \frac{1}{2} \left(\sin(2\omega t) + \sin(0) \right) \xrightarrow{qs} 0, \quad (12)$$

the volumetric damping power can be simplified to:

$$P_{d\Delta V,qs}(x, z) = \frac{\eta \omega^2 z^2}{2} \left[\left(\frac{\partial^2 \text{Re}\{\phi(x)\}}{\partial x^2} \right)^2 + \left(\frac{\partial^2 \text{Im}\{\phi(x)\}}{\partial x^2} \right)^2 \right] \quad (13)$$

The derived equation indicates that the damping is proportional to the square of the frequency and to the square of the distance from the beam center, meaning that the damping losses are expected mostly on the beam's surface.

2.2. Relationship between damping ratio and temperature increase

Eq. (13) uses the Kelvin-Voigt material model to show how the power of the dissipated energy is spatially distributed over a beam. To further validate this result, the spatial distribution is sought once again, but instead of using the Kelvin-Voigt model, a more general energy-based approach is utilized and related to the damping ratio.

Once again, the Euler-Bernoulli beam theory is considered. For such a vibrating beam, its strain energy is given as [12]:

$$W_l = \frac{1}{2} \int_0^l E I \left(\frac{\partial^2 \phi(x)}{\partial x^2} \right)^2 dx \quad (14)$$

$E I$ denotes the flexural rigidity and l is the length of the beam. The strain energy modal shape is considered [13], which can be written for an arbitrary interval $[a,b]$ on the beam as:

$$W_{ab} = \frac{1}{2} \int_a^b E I \left(\frac{\partial^2 \phi(x)}{\partial x^2} \right)^2 dx \quad (15)$$

When the interval is shortened towards zero, Eq. (15) yields an expression for the strain energy density $W(x)$:

$$W(x) = \frac{1}{2} E I \left(\frac{\partial^2 \phi(x)}{\partial x^2} \right)^2 \quad (16)$$

While the beam is vibrating, the total energy equals the sum of the consistently changing strain and kinetic energies. If the beam is observed under steady-state conditions, $\partial \phi(x)/\partial t = 0$, then the strain energy equals the total energy of the vibrating beam and $W(x)$ becomes the total energy density.

In cases when the damping ratio δ is low ($\delta \ll 1$), the damping can be characterized by Eq. (17), either as a ratio of the lost energy during a single cycle and the total energy of vibration, denoted by Ψ , or as a logarithmic ratio of the amplitudes of successive cycles [2].

$$\frac{\Delta W}{W} = \Psi = 2\delta = 2 \ln \frac{z_n}{z_{n+1}} \quad (17)$$

Here, ΔW represents the energy scattered in a single cycle, and z_n is the amplitude of vibration in the n -th cycle.

This research examines a homogeneous beam with a constant cross-section. The shape of $\phi(x)$ is not dependent on the amplitude of vibration z_n . This means that the ratio z_n/z_{n+1} is constant for every x and thus the Ψ and δ are also constant for every x . Since the energy density $W(x)$ depends on x

and Ψ does not, the energy scattered in each cycle must also depend on x : $\Delta W = \Delta W(x)$. Eqs. (16) and (17) yield:

$$\Delta W(x) = \delta EI \left(\frac{\partial^2 \phi(x)}{\partial x^2} \right)^2 \quad (18)$$

Regardless of the microscopic nature of the damping mechanisms, some of the energy dissipated by damping gets converted to heat. Next, the damping heat coefficient r is defined, which is the ratio of the energy that is being converted to heat and the total energy dissipated as a result of damping:

$$r = \frac{\Delta W(x)_{\text{heat}}}{\Delta W(x)} \quad (19)$$

The part of the energy that is being dissipated as heat results in an increase of the temperature:

$$\Delta W(x)_{\text{heat}} = m_u c \Delta T(x) \quad (20)$$

where c is the specific heat of the material, m_u denotes the mass per unit length of the beam and ΔT is the increase in the temperature after a single cycle.

Now, using Eqs. (18), (19) and (20) the relation between the damping ratio, the damping heat coefficient r and the temperature increase can be formed:

$$\Delta T(x) = \frac{r \delta E I}{c m_u} \left(\frac{\partial^2 \phi(x)}{\partial x^2} \right)^2 \quad (21)$$

Eq. (21) can be used to predict the temperature increase after a single cycle, if the damping ratio is known. Alternatively, it can be used to assess the damping ratio if the temperature increase has been measured. In both cases, the proportion of scattered energy converted to heat has to be known.

To calculate the temperature increase using Eq. (21), a second derivative of the operational deflection shape ϕ has to be calculated. In cases of proportionally damped materials, all the points on the beam move synchronously with the phase shift of either π or 0 [14]. With a damped polymer material, a phase shift and complex operational deflection shapes may arise. The strain energy of the beam from Eq. (16) will equal the total energy if the kinetic energy is 0 and the deflection is maximal. To identify those moments in time, the absolute value of complex shapes is used. Because of linearity, the square of the second derivative is expressed as the sum of squares of the second derivatives of the real and imaginary parts:

$$\left(\frac{\partial^2 \phi(x)}{\partial x^2}\right)^2 = \left(\frac{\partial^2 \text{Re}(\phi(x))}{\partial x^2}\right)^2 + \left(\frac{\partial^2 \text{Im}(\phi(x))}{\partial x^2}\right)^2 \quad (22)$$

Combining Eqs. (21) and (22) yields the final equation for the predicted temperature increase:

$$\Delta T(x) = \frac{r \delta E I}{c m_u} \left[\left(\frac{\partial^2 \text{Re}(\phi)}{\partial x^2}\right)^2 + \left(\frac{\partial^2 \text{Im}(\phi)}{\partial x^2}\right)^2 \right] \quad (23)$$

Notice that Eq. (23) proposes the same x dependency as Eq. (13), but instead of relating viscosity and power it directly relates the damping ratio and temperature increase over a single cycle.

2.3. Other drains of energy

This work focuses primarily on the part of the dissipated energy that is converted to heat; however, another very common drain of energy, acoustic radiation, is briefly presented here.

The sound power radiated from a vibrating surface can be determined as [15]:

$$P_s = \sigma_r \rho_a c_a S \bar{v}^2, \quad (24)$$

where σ_r is the radiation efficiency, $\rho_a c_a$ is the specific acoustic impedance of the fluid, S is the vibrating surface area and \bar{v}^2 is the mean square surface-averaged velocity.

A point on the beam's surface is vibrating according to Eq. (4). By deriving the beam deflection over time, the surface velocity can be obtained as:

$$\dot{w}(x, t) = v(x, t) = \omega \left(-\operatorname{Re}\{\phi(x)\} \sin(\omega t) + \operatorname{Im}\{\phi(x)\} \cos(\omega t) \right), \quad (25)$$

the time average of the squared surface velocity is:

$$\bar{v}^2(x) = \frac{\omega^2}{2} \left(\operatorname{Re}\{\phi(x)\}^2 + \operatorname{Im}\{\phi(x)\}^2 \right), \quad (26)$$

and the acoustically radiated power as

$$P_s = \sigma_r \rho_a c_a S \frac{\omega^2}{2} \left(\operatorname{Re}\{\phi(x)\}^2 + \operatorname{Im}\{\phi(x)\}^2 \right) \quad (27)$$

3. Experiment

A solid beam measuring $5 \times 20 \times 300$ mm made of polymethyl methacrylate (PMMA) was used. The beam was coated with highly emissive black paint that aided the measurements with a thermal camera. The measurement setup is shown in Fig. 2. The beam was excited using a LDS V406 shaker. The orientation of the beam was such that it was excited parallel to its shortest

dimension. The shaker and the beam were attached at a single point, 112 mm from the edge of the beam. A stinger connected the shaker and the beam, that reduced the thermal conduction and insulated the beam. The tested beam was surrounded by a cardboard shield which protected against radiation. Before each test, the specimen was thermically stabilized for 30 minutes.

The thermocamera used to measure the thermal field was the Deltatherm 1560 by Stressphotonics, equipped with a 320×256 focal plane array (FPA) sensible in the near-IR window, typical of InSb sensors. The FPA is refrigerated to 78K to minimize the noise-equivalent temperature value up to 18mK. The measurement system acquires up to 1000 FPS (frames per second), depending on the shutter settings. In the set up used for the experiments a 3.2 ms shutter and 100 FPS were set.

The beam was excited by a harmonic signal of a single frequency and constant amplitude. The test was performed close to two natural frequencies: the first test was performed at a frequency of 2225 Hz and the second at a frequency of 5530 Hz. To achieve steady-state temperature conditions, the samples were excited for 180 seconds. During the test, the thermal camera was continuously recording the temperature along the entire length of the tested beam. However, for later analysis only the last 2 seconds of the temperature maps [16] were integrated for 2 seconds to minimize the noise.

Later, white stripes were painted on the beam to provide a pattern for an optical measurement of the operational deflection shape (ODS). The vibrating beam was filmed with a Photron Fastcam SA-Z high-speed camera positioned at an angle to the beam's front surface to measure the bending

of the beam, see Fig. 2. Filming was performed at 50000 FPS, 12 bits of intensity resolution, a frame size of 1024×72 and 600,000 frames were captured. Using a gradient-based Optical Flow displacement amplitudes in the range of ten thousandths of a pixel can be measured [17]. The displacement was measured in a grid of 8×986 points. The obtained displacements were transformed to the frequency domain and only the excited harmonic was observed. The 8 lines of displacements were averaged to produce the ODS seen in Fig. 3. Each ODS (at 2225 and at 5530 Hz) was obtained from a separate measurement.

4. Results

4.1. Spatial comparison

According to Eq. (21), the generation of the heat and thus the temperature increase should be the highest at the points where the second derivative of deflection shape $\phi(x)$ is the highest. While the measured operational deflection shapes are shown in Fig. 3, the squared second spatial derivative of the measured deflection shapes (22) and the measured temperature increases after 180 seconds of excitation are shown in Fig. 4 and 5.

At the location of the excitation shaker, the theoretical equations for a Euler-Bernoulli beam (see Section 2) and discrepancies between the predicted and the measured temperatures are expected. Due to this reason, in Fig. 4 and 5 shows the location of the excitation shaker. Discrepancies can result from the heat being conducted through the stinger, either to or from the tested beam. Further, at the point of contact, heat might be generated due to friction or for other reasons that are not related to the damping of the observed structure.

4.2. Heating as a result of damping

After the correlation between the square of the second derivative and the temperature increase has been confirmed, theoretical values for the temperature increase can be calculated according to Eq. (21). Note that this equation yields the temperature increase in a single cycle. To obtain the temperature increase after an arbitrary time t , Eq. (21) has to be modified to:

$$\Delta T(x) = t f \frac{r \delta E I}{c m_u} \left(\frac{\partial^2 \phi}{\partial x^2} \right)^2 \quad (28)$$

where f is the vibration frequency in Hz.

As was discussed in Section 4, the sample was excited for 180 seconds. As the testing period is relatively long, heat transfer has to be taken into account when calculating the theoretical temperature increase. The heat transfer was modeled using the finite differences method [18]. Since the experimental results were averaged to yield a single value for each location x , the numerical simulation was also prepared for the longitudinal dimension of the beam, only. The beam was discretized into 986 elements of length Δx . The balance of the thermal energy was written for each element:

$$E_{gen} - E_{cond} - E_{conv} - E_{rad} = \frac{\Delta T}{c m_u \Delta x} \quad (29)$$

where E_{gen} is the thermal energy generated by damping, and E_{cond} , E_{conv} , E_{rad} are the energies drained from the element by conduction, convection and radiation, respectively. The thermal energy generated by damping on a discrete element was calculated as

$$E_{gen} = \Delta t f r \delta E I \left(\frac{\partial^2 \phi}{\partial x^2} \right)^2 \Delta x \quad (30)$$

The values of the parameters used for this numerical model can be found in Table 1.

With all the parameters known, the only unknown is the damping heat coefficient r introduced in Eq. (19). By comparing the theoretical results with the measured ones, the coefficient r can be estimated. In Fig. 6 the comparison between the numerical model using $r = 0.28$ and the measured temperature increase at the excitation frequency of 2225 Hz can be seen. For the excitation frequency at 5530 Hz $r = 0.32$ was used, see Fig. 7.

The results discussed in this research were obtained with a polymethyl methacrylate beam; it is worth noting that experiments with aluminum and steel beams were also performed, but due to the faster conduction in material, the temperature difference was at the limit of sensitivity of the measurement equipment.

When assessing other drains of energy, acoustic radiation has been considered (27). The major factor in accurately calculating the power that has been dissipated by acoustic radiation is the radiation efficiency σ_r . This factor is influenced by the dimension and shape of the object as well as the vibration frequency [15, 19], and thus reliably determining the σ_r is a challenge of its own and beyond the scope of this study. However, if the radiation efficiency σ_r is assumed to be 0.5 for both cases, the power dissipated by acoustic radiation is approximately 120 % of the thermally dissipated power in the 2225 Hz case and approximately 130 % of the thermally dissipated power in the 5530 Hz case.

5. Conclusion

This research investigated the relation between the damping of a vibrating system and the dissipation of energy in the form of heat. The theoretical background was derived and showed that the energy is not dissipated uniformly throughout the whole structure. Instead, heat and thus the temperature change correlates with the square of the second derivative of the operational deflection shape with respect to location. This hypothesis was tested experimentally, where it was shown that the temperature increase follows the predicted distribution.

Further, the research focuses on determining the proportion of dissipated energy, that is converted to heat. For this, the damping heat coefficient is introduced, which is the ratio between the dissipated energy that was converted to heat and the total energy that was dissipated as a result of the damping. For a polymethyl methacrylate beam it was experimentally shown that the damping heat coefficient is approximately 0.3. This means that approximately 30 % of the energy that is dissipated by the damping is converted into heat.

Acknowledgment

The authors acknowledge the partial financial support from the Slovenian Research Agency (research core funding No. P2-0263 and J2-6763).

- [1] J. Woodhouse, Linear damping models for structural vibration, *Journal of Sound and Vibration* 215 (3) (1998) 547–569.
- [2] A. Puškár, *Internal friction of materials*, Cambridge Int Science Publishing, Hertford, 2001.

- [3] M. Mihalec, J. Slavič, M. Boltežar, Synchrosqueezed wavelet transform for damping identification, *Mechanical Systems and Signal Processing* 80 (2016) 324–334.
- [4] A. D. Nashif, D. I. Jones, J. P. Henderson, *Vibration damping*, John Wiley & Sons, New York, 1985.
- [5] D. I. Jones, *Handbook of viscoelastic vibration damping*, John Wiley & Sons, New York, 2001.
- [6] X. Zhou, D. Yu, X. Shao, S. Zhang, S. Wang, Research and applications of viscoelastic vibration damping materials: A review, *Composite Structures* 136 (2016) 460–480.
- [7] S. Joshi, S. Hung, S. Vengallatore, Design strategies for controlling damping in micromechanical and nanomechanical resonators, *EPJ Techniques and Instrumentation* 1 (1) (2014) 1–14.
- [8] A. N. Norris, D. M. Photiadis, Thermoelastic relaxation in elastic structures, with applications to thin plates, *The Quarterly Journal of Mechanics and Applied Mathematics* 58 (1) (2005) 143–163.
- [9] R. Solecki, R. J. Conant, *Advanced mechanics of materials*, Oxford University Press on Demand, London, 2003.
- [10] S. S. Rao, *Mechanical vibrations*, 5th Edition, Pearson, Miami, 2011.
- [11] D. J. Ewins, *Modal testing: theory and practice*, Letchworth: Research studies press, Letchworth, 1984.

- [12] P. Cornwell, S. W. Doebling, C. R. Farrar, Application of the strain energy damage detection method to plate-like structures, *Journal of Sound and Vibration* 224 (2) (1999) 359–374.
- [13] E. Sazonov, P. Klinkhachorn, Optimal spatial sampling interval for damage detection by curvature or strain energy mode shapes, *Journal of Sound and Vibration* 285 (4) (2005) 783–801.
- [14] Z.-F. Fu, J. He, *Modal analysis*, Butterworth-Heinemann, Oxford, 2001.
- [15] F. Fahy, J. Walker, *Fundamentals of noise and vibration*, CRC Press, London, 1998.
- [16] R. Marsili, A. Garinei, Thermoelastic Stress Analysis of the contact between a flat plate and a cylinder, *Measurement* 52 (2014): 102-110.
- [17] J. Javh, J. Slavič, M. Boltežar, The subpixel resolution of optical-flow-based modal analysis, *Mechanical Systems and Signal Processing* 88 (2017) 89–99.
- [18] N. Ozisik, *Finite difference methods in heat transfer*, CRC press, Boca Raton, 1994.
- [19] G. Squicciarini, D. Thompson, R. Corradi, The effect of different combinations of boundary conditions on the average radiation efficiency of rectangular plates, *Journal of Sound and Vibration* 333 (17) (2014) 3931–3948.
- [20] M. Assael, S. Botsios, K. Gialou, I. Metaxa, Thermal conductivity of

polymethyl methacrylate (pmma) and borosilicate crown glass bk7, International Journal of Thermophysics 26 (5) (2005) 1595–1605.

List of Tables

1	Parameters used in the theoretical estimation, partially from [20]	19
---	---	----

Table 1: Parameters used in the theoretical estimation, partially from [20]

Parameter	Symbol	Value	Unit
Thermal conductivity	λ	0.192	$\text{W m}^{-1} \text{K}^{-1}$
Heat capacity	c	1466	J K^{-1}
Emissivity	ϵ	0.98	1
Young's modulus	E	1944	MPa
Density	ρ	1170	kg m^{-3}
Discrete time interval	Δt	0.01	s
Discrete position interval	Δx	0.3	mm
Damping ratio at 2225 Hz	δ_{2225}	0.025	1
Damping ratio at 5530 Hz	δ_{5530}	0.020	1
Radiation efficiency	σ_r	0.5	1
Specific acoustic impedance of air	$\rho_a c_a$	413.3	Pa s m^{-3}

List of Figures

1	The Kelvin-Voigt material model	21
2	Measurement setup	22
3	Measured operational deflection shapes at 2225 Hz and 5530 Hz.	23
4	Measured temperature increase and the square of the second derivative of the measured deflection shape at 2225 Hz.	24
5	Measured temperature increase and the square of the second derivative of the measured deflection shape at 5530 Hz.	25
6	Theoretical and experimental temperature increases at an excitation of frequency 2225 Hz.	26
7	Theoretical and experimental temperature increases at an excitation of frequency 5530 Hz.	27

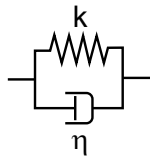


Figure 1: The Kelvin-Voigt material model

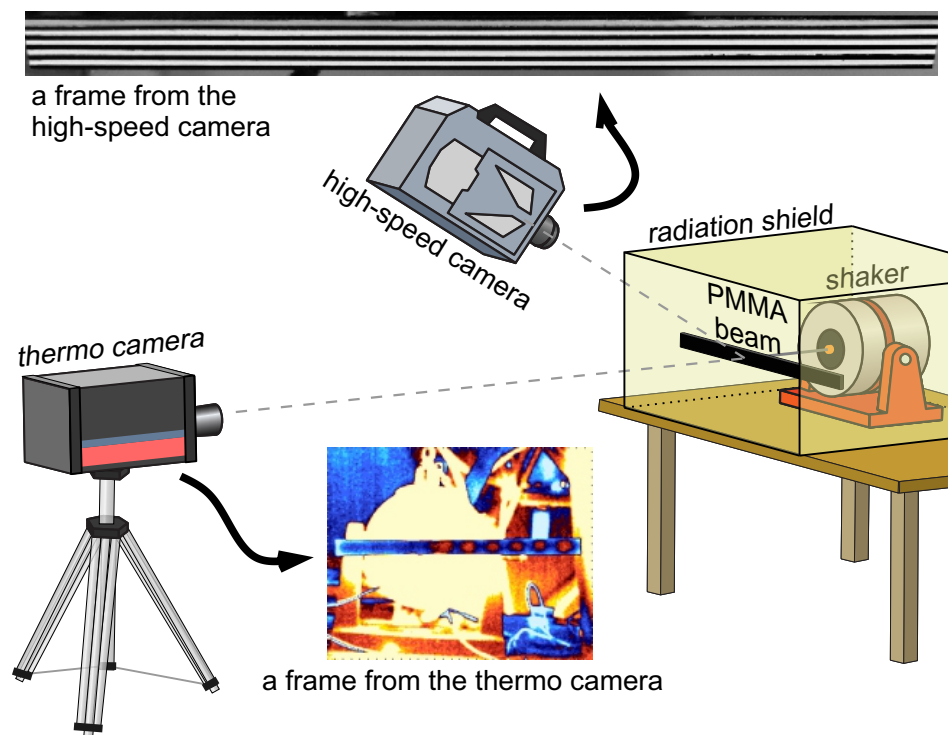


Figure 2: Measurement setup

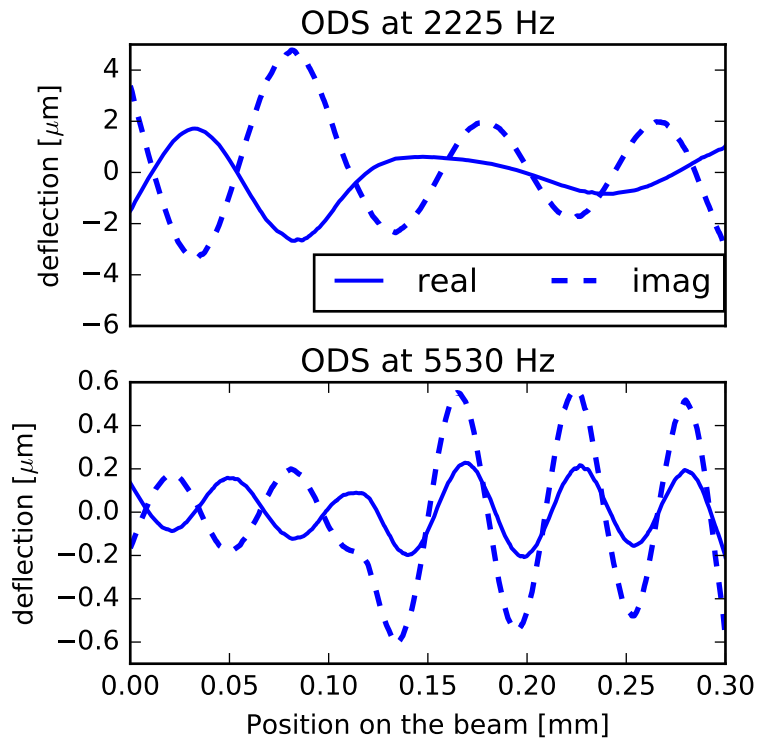


Figure 3: Measured operational deflection shapes at 2225 Hz and 5530 Hz.

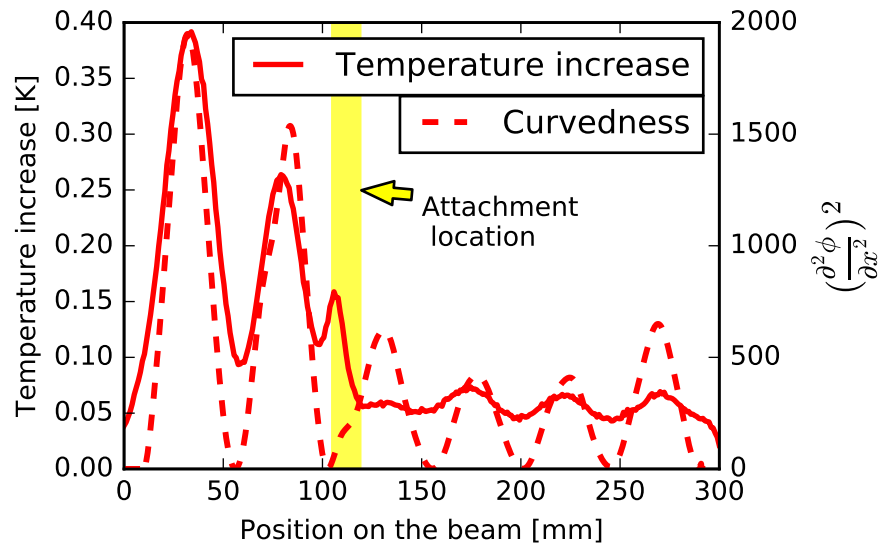


Figure 4: Measured temperature increase and the square of the second derivative of the measured deflection shape at 2225 Hz.

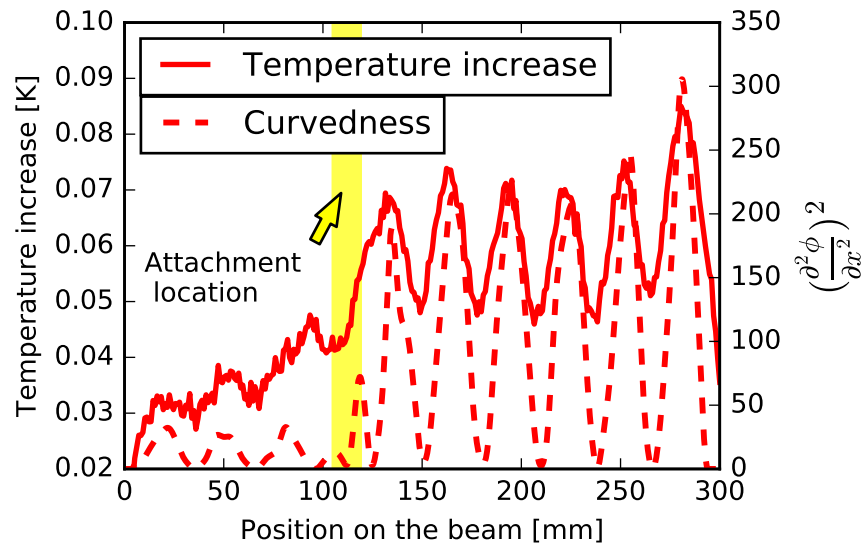


Figure 5: Measured temperature increase and the square of the second derivative of the measured deflection shape at 5530 Hz.

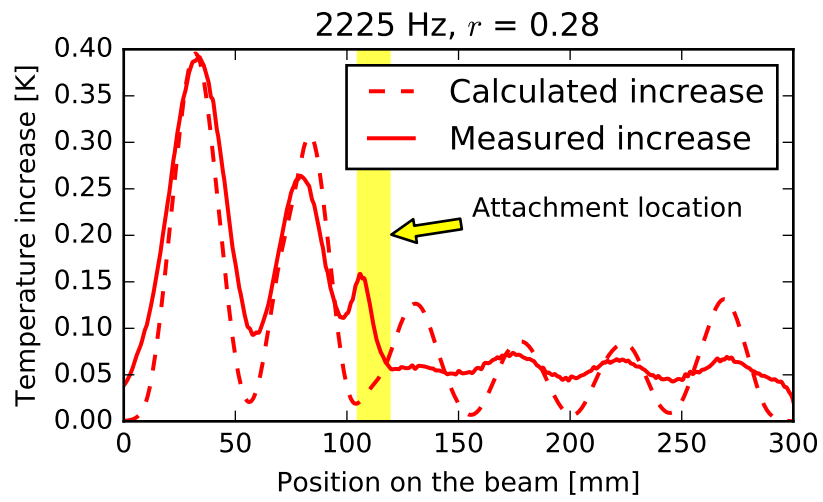


Figure 6: Theoretical and experimental temperature increases at an excitation of frequency 2225 Hz.

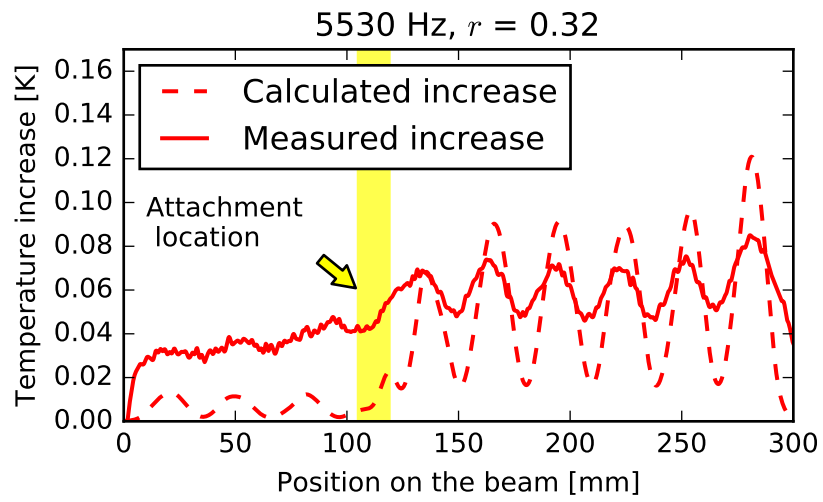


Figure 7: Theoretical and experimental temperature increases at an excitation of frequency 5530 Hz.